WATER RESOURCES RESEARCH, VOL. 26, NO. 7, PAGES 1517–1528, JULY 1990

Mathematical Modeling of Tracer Behavior in Short-Term Experiments in Fissured Rocks

PIOTR MALOSZEWSKI AND ANDRZEJ ZUBER[1]

Institut für Hydrologie, Gesellschaft für Strahlen-und Umweltforschung mbH München, Neuherberg, Federal Republic of Germany

Transport equations for a single fissure in a porous matrix are coupled with a chemical model allowing for both an instantaneous equilibrium governed by a linear adsorption isotherm and a nonequilibrium kinetic reaction of the first order. The fitting procedure of the obtained solution is improved by additional fitting of the mass recovery curves; i.e., the fitting consists of a trial-and-error procedure applied in turn to the concentration tracer curve and the mass recovery curve until a given set of parameters gives the best fit of both theoretical curves to the experimental data. The model is tested against known multitracer experimental data from a fissured chalk formation. It is shown how some physical parameters can be obtained by a combined interpretation of the tracer and pumping data. However, in the case of adsorbable tracers some of the parameters must be known from a nonsorbable tracer experiment. In spite of its approximate nature the model works surprisingly well for nonsorbable tracers and reasonably well for sorbable solutes.

INTRODUCTION

The movement of solutes in fissured rocks has attracted a lot of attention since the early works of *Grisak and Pickens* [1980], *Grisak et al.* [1980], and *Neretnieks* [1980], though most of the authors concentrated on the movement of continuously injected pollutants. *Maloszewski and Zuber* [1985] showed that in short-term tracer experiments the mathematical model of diffusion from a single fissure to the microporous matrix yields satisfactory estimates of the water flow velocity, in spite of a different behavior of the tracer and the traced mobile water. In a recent work, *Maloszewski and Zuber* [1989] interpreted a multitracer experiment of *Garnier et al.* [1985] with the aid of the single-fissure dispersion model, assuming for an adsorbable tracer ($H^{13}CO_3^-$) an instantaneous equilibrium between the solid and liquid phases in the matrix, governed by the linear adsorption isotherm. The parameters obtained were much more internally consistent and logical than those from the original interpretation of *Garnier et al.* [1985], though still not free of some ambiguities, because the dispersivity obtained from the $H^{13}CO_3^-$ tracer curve differed considerably from that obtained from other tracer curves (D_2O, I^-, and uranine). In this paper it is shown how a proper normalization (concentration divided by mass or activity injected) exhibits differences between particular tracer curves, which result from diffusion into the matrix and possible interaction with the solid phase. In comparison with our earlier works a more refined model of adsorption is applied, which includes for the matrix both an instantaneous equilibrium governed by a linear adsorption isotherm and the first-order nonequilibrium kinetic reaction. In order to avoid too much complexity the tracer adsorption on fissure walls is approximated only by instantaneous equilibrium governed by a linear adsorption isotherm. The interpretation is also improved by additional fitting of the theoretical mass recovery curves (cumulative tracer curves) to the experimental data, which according to *Klotz et al.* [1988] is particularly suitable for the interpretation of adsorable tracers.

THE GENERAL MODEL

It has been shown that the transport of solutes in fissured rocks with a porous matrix may be approximated by the dispersion equation formulated for a system of parallel fissures coupled with the diffusion equation in the matrix [*Sudicky and Frind*, 1982; *Maloszewski and Zuber*, 1985]. In the case of adsorbable solutes, additional equations are needed to describe the assumed adsorption model. In this work the following governing equations are used.

For solute transport in water in the fissures,

$$R_{af}\frac{\partial c_f}{\partial t}+v\frac{\partial c_f}{\partial x}-D\frac{\partial^2 c_f}{\partial x^2}-\frac{n_p D_p}{b}\frac{\partial c_p}{\partial y}\Big|_{y=b}=0 \qquad (1)$$

For solute transport in water in the matrix,

$$n_p\frac{\partial c_p}{\partial t}+(1-n_p)\rho(\Phi_1+\Phi_2)-n_p D_p\frac{\partial^2 c_p}{\partial y^2}=0 \qquad (2)$$

For solute distribution between the water and solid phases of the matrix,

$$\Phi_1=\frac{\partial q_1}{\partial t}=k_3\frac{\partial c_p}{\partial t} \qquad (3)$$

$$\Phi_2=\frac{\partial q_2}{\partial t}=k_1\frac{n_p c_p}{(1-n_p)\rho}-k_2 q_2 \qquad (4)$$

where c_f and c_p are the solute concentrations per unit volume of water in the fissures and matrix, respectively, t is the time variable, x is the spatial coordinate taken in the direction of flow, y is the spatial coordinate perpendicular to the fissure extension, v is the mean water velocity in the fissures, D is the dispersion coefficient in the fissures, n_p is the matrix porosity, D_p is the molecular diffusion coefficient in the matrix, b is the half-fissure aperture, ρ is the density of matrix material, Φ_1 is the mass transfer of solute between

[1]On leave from Institute of Nuclear Physics, Cracow, Poland.

Paper number 90WR00352.
0043-1397/90/90WR-00352$05.00

the liquid and solid phases in the matrix governed by a linear adsorption isotherm and an instantaneous equilibrium, Φ_2 is the mass transfer of solute between the solid and liquid phases in the matrix governed by a first-order nonequilibrium kinetic reaction, q_1 and q_2 are the partial solute concentrations in the solid phase expressed per unit weight of the solid material, k_3 is the distribution coefficient for an instantaneous equilibrium expressed in units of volume per unit weight of the solid material, k_1 and k_2 are the forward and backward rate constants for nonequilibrium kinetic reaction, respectively, and R_{af} is the retardation factor in the fissures resulting from an equation similar to (3) but formulated for the fissures.

It will be recalled that convective flow in the matrix is equal to zero and that the tracer distribution across the fissure width is constant as a result of sufficient transverse dispersion and diffusion. A decay term is omitted, which means that considerations of this paper are limited to nondecaying solutes or to radioisotopes instantaneously injected and corrected for the radioactive decay. When (1) is applied to a groundwater system containing more than one fissure, b is the effective half-fissure aperture, and D is the effective dispersion coefficient resulting from the spectrum of velocities in fissures. If the fissures are not interconnected, the dispersion coefficient will be proportional to both the velocity and distance; i.e., the dispersivity, D/v, will be proportional to the distance, which imposes some limitations on the applicability of the dispersion model. If the fissures are interconnected and the scale of an experiment is large enough, the dispersivity will probably reach an asymptotic value, and the model should be less restricted.

The liquid-solid phase reaction model of (2)–(4) is that developed by *Cameron and Klute* [1977] for granular media and successfully applied by *Klotz et al.* [1988] for modeling ^{85}Sr transport in sands.

THE BOUNDARY AND INITIAL CONDITIONS

The conditions for which (1)–(4) were solved are as follows:

$$c_f(x, 0) = 0 \tag{5a}$$

$$c_f(0, t) = (M/Q)\delta(t) \tag{5b}$$

$$c_f(\infty, t) = 0 \tag{5c}$$

$$c_p(y, x, 0) = 0 \tag{5d}$$

$$c_p(b, x, t) = c_f(x, t) \tag{5e}$$

$$c_p(\infty, x, t) = 0 \tag{5f}$$

$$q_1(x, 0) = 0 \tag{5g}$$

$$q_2(x, 0) = 0 \tag{5h}$$

where M is the mass or activity of tracer instantaneously injected, Q is the volumetric flow rate through the system, and $\delta(t)$ is the Dirac delta function. Equation (5*b*) defines the tracer concentration in the so-called flux concentration term [e.g., *Kreft and Zuber*, 1978, 1986], whereas in (5*e*) both concentrations should be expressed in terms of resident concentration. However, if $D/(vx) < 0.1$, both concentrations are practically the same. Equation (5*f*) defines the single-fissure approximation which has been shown by *Maloszewski and Zuber* [1985] to be valid for short-term tracer experiments. Such an experiment is defined as that in which the tracer has insufficient time to penetrate the matrix deeply enough to be influenced by the adjacent fissures. Examples given by *Maloszewski and Zuber* [1985] seem to suggest that experiments with a mean flow time up to 1 month are usually very well interpretable by the single-fissure approximation.

SOLUTION

The solutions of (1)–(4) with boundary conditions (5) are shown in the appendix. The concentration of tracer as a function of time for a given distance (x) reads as follows:

$$c_f(t) = \frac{aM}{2\pi Q}(Pe\ t_o')^{1/2} \cdot \left\{ \int_0^t \exp\left[-\frac{Pe}{4ut_o'}(t_o' - u)^2 - k_1'(t-u) - \frac{a^2u^2}{t-u} \right] \cdot \frac{du}{[u(t-u)^3]^{1/2}} + (k_1'k_2)^{1/2} \cdot \int_0^t \exp\left[-\frac{Pe(t_o' - u)^2}{4ut_o'} - k_1'(t-u) \right] u^{-1/2} \cdot \int_u^t \exp\left[-\frac{(au)^2}{(\tau - u)} - (k_1' - k_2)(\tau - t) \right] \cdot I_1[4k_1'k_2(\tau - u)(t-\tau)]^{1/2} \frac{d\tau}{\tau - u} \frac{du}{(t-\tau)^{1/2}} \right\} \tag{6}$$

where

$$k_1' = k_1/R_{ap} \tag{7}$$

$$R_{ap} = (1 - n_p)\rho k_3/n_p \tag{8}$$

$$a = n_p R_{ap}(D_p/R_{ap})^{1/2}/(2bR_{af}) = n_p(D_p R_{ap})^{1/2}/(2bR_{af}) \tag{9}$$

$$Pe = vx/D \tag{10}$$

$$t_o' = xR_{af}/v = R_{af}t_o \tag{11}$$

where t_o is the mean transit time of water (x/v or V/Q, where V is the mobile water volume in the system and Q is the volumetric flow rate through it) and Pe is the Peclet number.

The fitting (sought) parameters of the model are a, t_o', Pe, k_1', and k_2, whereas the departure parameters are t_o or v, D/v, R_{ap}, R_{af}, k_1, k_2, D_p, n_p, and $2b$. The number of fitting parameters in (6), in comparison with the number of departure parameters having a direct physical meaning, is reduced by applying (7), (9), and (11). This solution is called here generally the single-fissure dispersion model (SFDM).

In the case of $\Phi_2 = 0$, i.e., $k_1 = k_2 = 0$, (6) simplifies to

$$c_f(t) = \frac{Ma}{2\pi Q}(Pe\ t_o')^{1/2} \cdot \int_0^t \exp\left[-\frac{Pe(t_o' - u)^2}{4ut_o'} - \frac{a^2u^2}{t-u} \right] \frac{du}{[u(t-u)^3]^{1/2}} \tag{12}$$

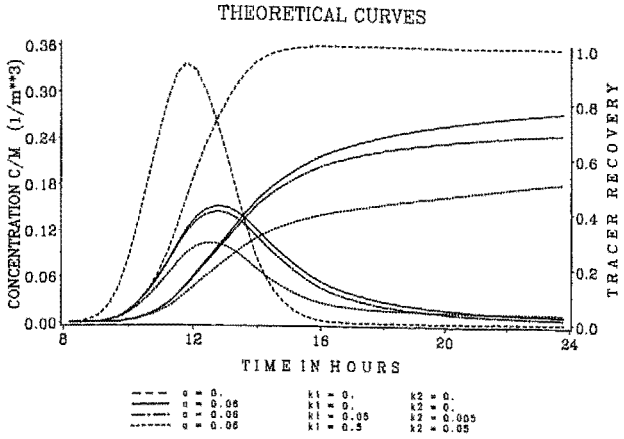

Fig. 1. An example of theoretical tracer concentration and mass recovery curves for $t_o = 12$ hours and $Pe = 0.005$ in the case of no diffusion and no adsorption ($a = 0$, $R_{af} = R_{ap} = 1$, $k_1 = k_2 = 0$), diffusion without adsorption ($a > 0$, $R_{af} = R_{ap} = 1$, $k_1 = k_2 = 0$), and diffusion with kinetic adsorption ($a > 0$, $R_{af} = R_{ap} = 1$, $k_1 > 0$, $k_2 > 0$) (a is in hours$^{-1/2}$, k_1 and k_2 in hours^{-1}).

which is equivalent to (15) in the work by *Maloszewski and Zuber* [1985] but has a much more convenient form for numerical calculations. The fitting parameters of this model are t_o', a, and Pe, whereas the departure parameters are t_o, Pe, R_{ap}, R_{af}, D_p, n_p, and $2b$.

In Figure 1 an example is shown to demonstrate how the model works in comparison with the case of no diffusion into the matrix ($a = 0$). In the case of diffusion without adsorption the tracer curves are lower and shifted to longer times in comparison with the curves in the no-diffusion case. If the rate constants differ from zero, the tracer peaks are further reduced in comparison with the case of no adsorption, and the tail is prolonged. However, for the low values of k_1 and k_2 shown in Figure 1 the position of maximum concentration may be shifted to earlier times in comparison with the case of no adsorption. For large values of k_1 and k_2 a reversal shift to greater times is observed (not shown here). The mass recovery curves, obtained by numerical integration of (6) or (12), are also shown. These curves give a better insight into the behavior of tracers at the tailing parts and allow for the discovery of nonreversible losses, as will be shown later.

Discussion of Parameters

For an ideal tracer, $R_{af} = R_{ap} = 1$ and $k_1 = k_2 = 0$. In such a case, as mentioned earlier, there are three fitting parameters, $t_o' = t_o$, Pe, and a, where according to (9), a is then given as

$$a = n_p(D_p)^{1/2}/(2b) \tag{13}$$

which means that if a is found from a tracer experiment and if n_p and D_p are obtained from laboratory measurements on core samples, the fissure width $2b$ is directly determinable from that formula.

Another approach proposed by *Maloszewski and Zuber* [1985] is applicable in the case of a tracer experiment combined with a pumping test [*Zuber*, 1974]. In such a case, if the volume of the depression cone is negligible in comparison with the volume of water in the investigated part of the system (i.e., water in the cylinder of radius x and height h), the fissure porosity n_f is given as

$$n_f = (Qt_o)/(\pi h x^2) \tag{14}$$

where Q is the volumetric pumping rate, h is the thickness of the aquifer, and x is the distance between the wells. The fissure porosity, in turn, may serve for estimation of the fissure width for a given model of the fissure network. For instance, for a model of a network of tortuous fissures of the same width the following formula was obtained [*Zuber*, 1974]:

$$K = n_f(2b)^2/(12\tau_f^2) \tag{15}$$

where K is the permeability coefficient and τ_f is the tortuosity factor for fissures. Equation (15) is very close to equations derived for a network of capillaries [*Saffman*, 1959] or for a network of tortuous capillaries [*Pirson*, 1963]. This equation may be rearranged to a more practical form,

$$2b = \tau_f(k_{10}/n_f)^{1/2}/2330 \tag{16}$$

where $2b$ is expressed in centimeters and k_{10} is the hydraulic conductivity at 10°C expressed in meters per day.

The matrix porosity n_p can be found from (13) by putting [*Neretnieks*, 1980]

$$D_p = n_p\delta D_v/\tau_p \tag{17}$$

where δ is the constrictivity which depends on pore and diffusing component sizes, τ_p is the tortuosity factor for the matrix, and D_v is the coefficient of diffusion in free water. Substituting (17) into (13) gives

$$n_p = [(2ba)^2\tau_p/(\delta D_v)]^{1/3} \tag{18}$$

for a nonsorbing substance (ideal tracer). However, if the diffusion coefficient in the matrix is sought from (13), the matrix porosity has to be known independently.

For reactive tracers the number of fitting parameters is so large that no unambiguous interpretation is possible without a prior determination of t_o, a, and Pe from an ideal tracer experiment. When a good fit is also obtained for a reactive tracer curve, the R_{af} factor can be found by comparison of t_o' with t_o, whereas R_{ap} can be found by comparison of the values of the a parameter obtained from both curves if the D_p values for both tracers are known. The rate constants, k_1 and k_2', are determined directly. It remains unknown if the field values of the reaction parameters can be predicted from laboratory batch or column experiments. However, for a better understanding of the physical meaning of the reaction parameters the following formulas may be used.

The R_{af} factor is expressed as [e.g., *Freeze and Cherry*, 1979; *Maloszewski and Zuber*, 1985]

$$R_{af} = 1 + k_a/b \tag{19}$$

where k_a is defined as the distribution coefficient for the concentration in the solid phase, q_s, expressed per unit rock surface,

$$k_a = (q_s/c_f)_{\text{equilibrium}} \tag{20}$$

According to (19), for a large fissure aperture the R_{af} factor is close to 1, but for a strongly adsorbed tracer and a very

thin fissure it may differ from 1. Its estimation requires the measurement of k_a and b.

In order to be consistent with the previous notation, (19)–(22) should be understood as applicable for an instantaneous equilibrium. However, they are also applicable for the asymptotic equilibrium represented later by (23).

Under an assumption of a microporous matrix consisting of a set of parallel and equal diameter (d_c) capillaries, the R_{ap} factor can be expressed as [*Maloszewski and Zuber*, 1985]

$$R_{ap} = 1 + 4k_a/d_c \tag{21}$$

The distribution coefficient defined for a hard rock, or more generally for any geometrical form of the material, can be related to the distribution coefficient (k_3 or k_d) measured on the fine ground material consisting of spheres by [*Maloszewski and Zuber*, 1985]

$$k_a = \tfrac{1}{3}\rho k_d \left(\sum_{i=1}^{j} \frac{v_i}{r_i} \right)^{-1} \tag{22}$$

where the grain size curve of the ground material is divided into j groups of weight fractions, v_i, and the radii of r_i.

It is evident that whereas some estimate of k_a is possible, an independent determinations of R_{ap} requires also the microscope observations of the micropore dimensions and shape. In the case of a simple model given by (21) it is sufficient to know the diameter of the micropores.

The reaction parameters, k_1, k_2, and k_3, are related to the commonly known distribution coefficient, k_d, by the following formula:

$$k_d = k_3 + \frac{n_p}{(1 - n_p)\rho} \frac{k_1}{k_2} \tag{23}$$

which may be deduced from (3) and (4). The larger the k_1/k_2 ratio, the larger the k_d value, whereas an increase in both k_1 and k_2 leads to a faster equilibration.

It has to be remembered that (23) is valid only for a given system. For a transfer of the reaction parameters obtained in laboratory experiments on a granular material to hard rock in the field, or vice versa, a model relating the surface available for sorption with other parameters of the system is required, similar to that discussed above for an instantaneous equilibrium reaction. It is self-evident that batch experiments should not be limited to the determination of k_d values but should also cover observations of the reaction kinetics.

THE EXPERIMENTAL DATA

A unique opportunity to compare the behavior of different tracers and to validate our model is offered by the multitracer experiment performed by *Garnier et al.* [1985] in a fissured chalk formation overlain by clays and silts. The transmissivity of that chalk is (1.5–2.0) × 10^{-3} m^2/s (J. M. Garnier, private communication, 1987), which for the thickness of 32.8 m yields the hydraulic conductivity (4.6–6.1) × 10^{-5} m/s = 4.0–5.3 m/d. The injection well was screened over the depth of 19.9–29.9 m (10 m), and the pumping well situated at a distance of 10.22 m was screened over the depth of 19.17–34.17 m (15 m). The pumping was performed with the flow rate of 20.8 m^3/h. Four tracers, D_2O, I^-, uranine (disodium fluorescine), and $H^{13}CO_3^-$, were instantaneously

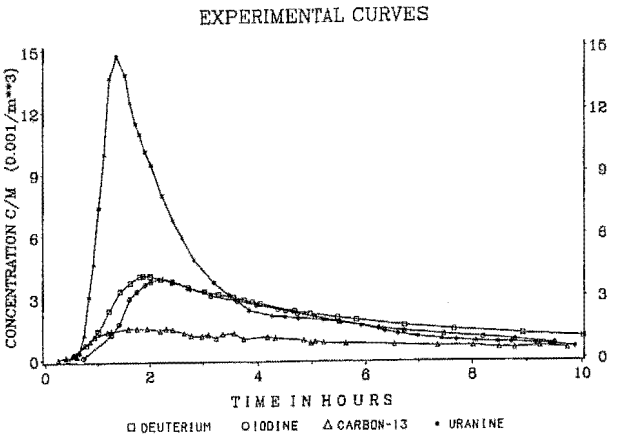

Fig. 2. Tracer curves of *Garnier et al.* [1985] normalized to the injected mass.

injected, and their concentrations measured in pumped water. The four tracer curves were presented by *Garnier et al.* [1985] in a very common but unfortunately very obscure method in which each curve is normalized to its maximum concentration value. The most proper way for comparing different tracer curves obtained in a single experiment is to normalize all the concentrations by dividing the measured concentration of a given tracer by its injected mass or activity. Such a normalization was done here by making use of the values of maximum concentrations and injected amounts of tracers given by *Garnier et al.* [1985]. Properly normalized tracer curves are shown in Figure 2. Unfortunately, the accuracy of the experimental data obtained in this way remains unknown. Nevertheless, it is quite clear that particular tracer curves differ considerably; this was not so visible when they were normalized to the maximum concentration. From the inspection of the curves shown, it may qualitatively be said that the highest peak for uranine results from a low-diffusion coefficient of that tracer and, in consequence, relatively small diffusion into and out of the matrix. Both heavy water (D_2O) and iodine have much lower peaks than uranine, probably as a result of higher values of diffusion coefficients and consequently greater diffusion into and out of the matrix. The iodine curve lies in the initial and tailing parts below the D_2O curve, which means that this tracer is to some degree adsorbed. On the other hand, $H^{13}CO_3^-$ is apparently strongly lost by sorption in the matrix. All these findings will be quantitatively verified further by the values of parameters obtainable from the developed model.

FITTING OF THE MODEL AND EVALUATION OF THE PARAMETERS

The model given by (1)–(4) and their solutions, (6) and (12), is valid for unidimensional flow, whereas the available experimental data were obtained in radial flow. However, there are physical reasons to expect the unidimensional model to work satisfactorily for the radial flow when the tracer is injected in a well situated within the radial symmetry of the depression cone and its concentration measured in the pumping well. These physical reasons are related to the convergence of flow lines in the pumping well, which diminishes the effects caused by transverse dispersion. Examples

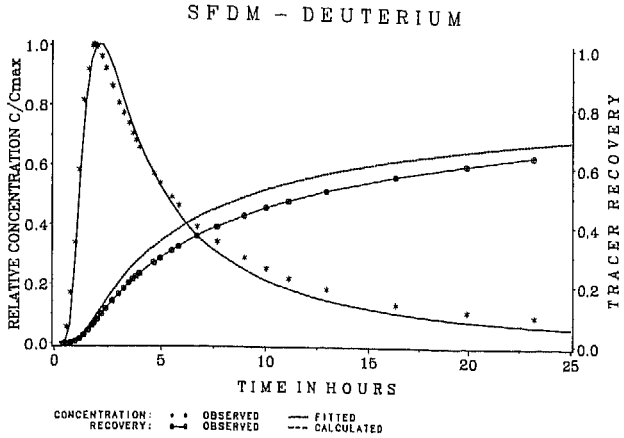

Fig. 3. Fitting of (12) for D_2O without fitting of the mass recovery curves (parameters given in Table 1).

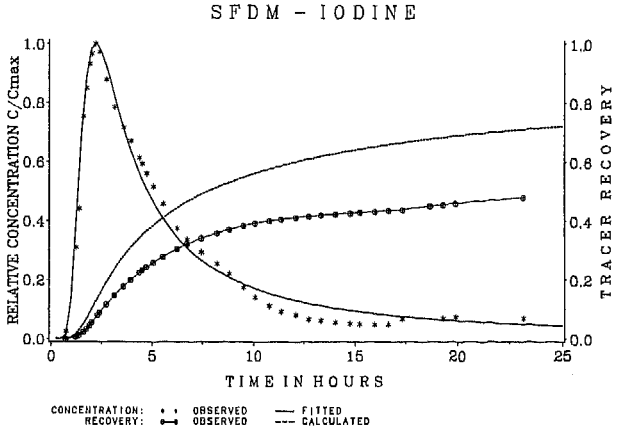

Fig. 5. Fitting of (12) for I^- without fitting of the mass recovery curves (parameters given in Table 1).

of a good fit of the unidimensional model and reasonable values of parameters reported in a number of papers seem to confirm such an approximation [e.g., *Lenda and Zuber*, 1970; *Zuber*, 1974; *Maloszewski and Zuber*, 1985]. A converging radial flow created by pumping is especially suitable for tracer experiments in fissured microporous rocks because it allows inclusion of the concept of mass recovery into the fitting procedure, which improves the interpretation, as will be further demonstrated.

Identification of Parameters

Making use of simple reaction model (equation (12)) without additional fitting of mass recoveries. Figures 3–6 show the experimental data of Figure 2 and the theoretical curves of "the best fit" for (12) in the case of normalization to the maximum concentration value, i.e., without taking the mass recovery into account. Parameter values are given in Table 1. *Maloszewski and Zuber* [1989] have already discussed the values of some parameters obtained from that interpretation and their internal consistency in comparison with the parameters estimated by *Garnier et al.* [1985]. The only inconsistency reported by *Maloszewski and Zuber* [1989] was in the value of the dispersivity obtained from the $H^{13}CO_3^-$ tracer curve, which differed considerably from the value obtained from all the other tracer curves (1.2 versus 0.3 m, respectively). A search for a better model, performed within this work, disclosed an additional inconsistency manifested by a lack of fitting for the mass recovery curves as demonstrated in Figures 3–6.

It should be noted that contrary to our earlier suggestion [*Maloszewski and Zuber*, 1989] the fit is not improved by the inclusion of a possible process of adsorption on the fissure wall because it changes only the physical meaning of two fitting parameters (t_o and a). If the differences in t_o values given in Table 1 are treated as differences between t_o and t'_o values, an unreasonable high R_{af} value is obtained, which, in turn, leads to an unreasonably high k_a value. Because of that the R_{af} factor was assumed to be equal to unity.

Within this work it was assumed that the micropores in the chalk are sufficiently large to ensure $\delta = 1$ and that $\tau_p = 1.5$. The following values of the diffusion coefficients D_v were used: 2.5×10^{-5} cm^2/s for D_2O, 4.5×10^{-6} cm^2/s for uranine [*Skagius and Neretnieks*, 1986], 1.6×10^{-5} cm^2/s for iodine [*Skagius and Neretnieks*, 1986], and 10^{-5} cm^2/s for $H^{13}CO_3^-$ (from the data reported by *Garnier et al.* [1985]).

It has to be stressed that the accuracy of the matrix porosity determination depends on the validity of assumptions related to the diffusion coefficients. Equation (18) is not applicable for finding n_p if $\delta < 1$.

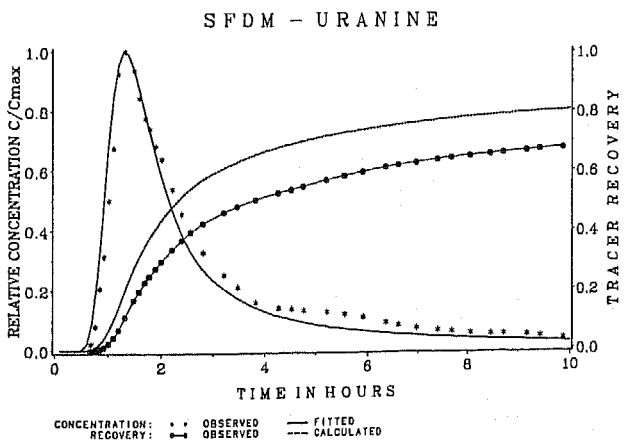

Fig. 4. Fitting of (12) for uranine without fitting of the mass recovery curves (parameters given in Table 1).

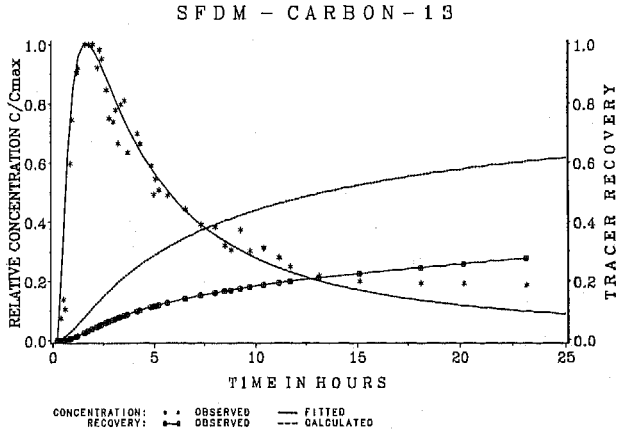

Fig. 6. Fitting of (12) for $H^{13}CO_3^-$ without fitting of the mass recovery curves (parameters given in Table 1).

TABLE 1. Parameters Obtained From Equation (12) Without Fitting of the Recovery and Assuming $R_{af} = 1.0$

Tracer	Fitted Parameters			Calculated Parameters			
	t_0, hours	Pe^{-1}	a, hours$^{-1/2}$	n_f,[a] %	$2b$,[b] μm	n_p,[c] %	R_{ap}
D_2O	1.0	0.03	1.4	0.19–0.42	200–570	26–47	1.0[d]
Uranine	1.15	0.03	0.45	0.22–0.49	180–530	18–37	1.0[d]
I^-	1.25	0.03	0.95	0.24–0.52	180–500	20–39	1.0[d]
$H^{13}CO_3^-$	0.90	0.12	2.0	0.17–0.38	210–600	36[d]	1.6–12.8[e]

[a]Equation (14).
[b]Equation (16).
[c]Equation (17) and (18).
[d]Assumed.
[e]Calculated from equations (9) and (17).

The ranges of parameters given in Table 1 result from taking the end values of known parameters of the formation (h = 15–32.8 m, k_{10} = 4.0–5.3 m/d, and τ_f = 1.5–2.5). For $H^{13}CO_3^-$ it is necessary to assume that the R_{ap} factor differs from unity. Its value was found from (9) and (17) with $\delta = 1$ for the mean matrix porosity estimated from other tracer data and for the extreme values of $2b$ determined from (9) for the D_2O tracer curve.

It is obvious from Table 1 that (12) does not work properly for $H^{13}CO_3^-$ because the Peclet number obtained from this tracer curve differs considerably from the values obtained for all the other tracer curves. It is also evident that the experimental mass recoveries for that tracer as well as for I^- are much lower than the values expected theoretically, which means that considerable amounts of these two tracers were lost. It should be noted that in spite of a common opinion, I^- is not quite a conservative tracer, as in accordance with other works [e.g., *Behrens*, 1985; *Maloszewski et al.*, 1980].

Additional fitting of mass recoveries and making use of a model combining instantaneous equilibrium and nonequilibrium kinetic reactions (equation (6)). As shown earlier, a simplified model represented by (12) yielded neither a consistent Pe value from the $H^{13}CO_3^-$ tracer curve nor proper mass recoveries especially for that tracer and I^-. A more refined model represented by (6) was used for the interpretation of these two tracers and additional fitting of the mass recoveries applied to all the tracer curves (Figures 7–10). The fitting consists of a trial-and-error procedure applied in turn to the concentration tracer curve and the mass recovery curve until a given set of parameters gives the best fit of both the theoretical curves to the experimental data. The fitting procedure is stopped when the sum of the squared differences between the theoretical and experimental values is at minimum.

Unfortunately, it was not possible to obtain a good fit without assuming that 9% of each tracer is missing; i.e., all the theoretical mass recovery curves had to be multiplied by 0.91. Most probably, 9% of the injected solution was trapped in the unscreened part of the injection well. For the sake of consistency the mass recovery curves given in Figures 3–6 were also corrected for the lost tracer.

The parameters obtained for all four tracers from the new interpretational procedure and the new model are summarized in Table 2. The most striking feature is the decrease of t_o and Pe^{-1} for D_2O and uranine in comparison with the values shown in Table 1, though in both cases the same model (equation (12)) was applied. This means that the fitting of mass recoveries improves the interpretational procedure considerably. It should be mentioned here that the normalization to the maximum concentration causes a loss of information on the mass recovery. It appears that in practice, a good fit of the concentration curves is a necessary, though not sufficient, condition for a good fit of the mass recovery. Therefore an additional fitting of the mass recovery curves improves the interpretation.

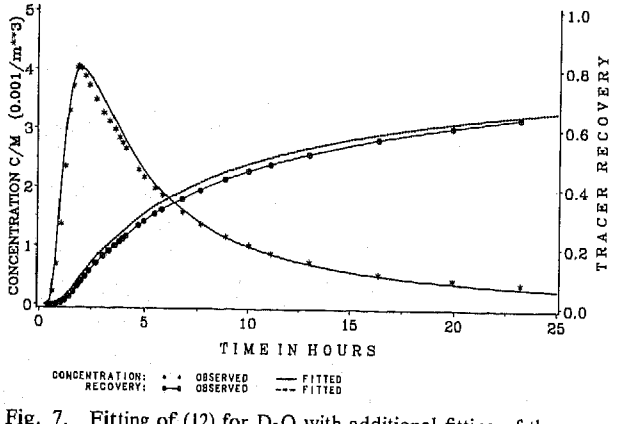

Fig. 7. Fitting of (12) for D_2O with additional fitting of the mass recovery curves (parameters given in Table 2).

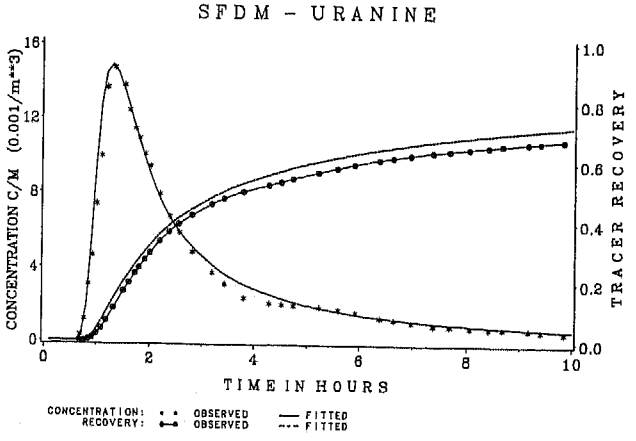

Fig. 8. Fitting of (12) for uranine with additional fitting of the mass recovery curves (parameters given in Table 2).

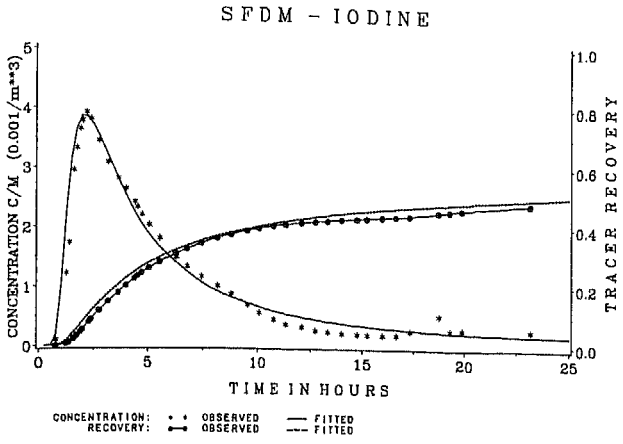

Fig. 9. Fitting of (6) for I^- with additional fitting of the mass recovery curves (parameters given in Table 2).

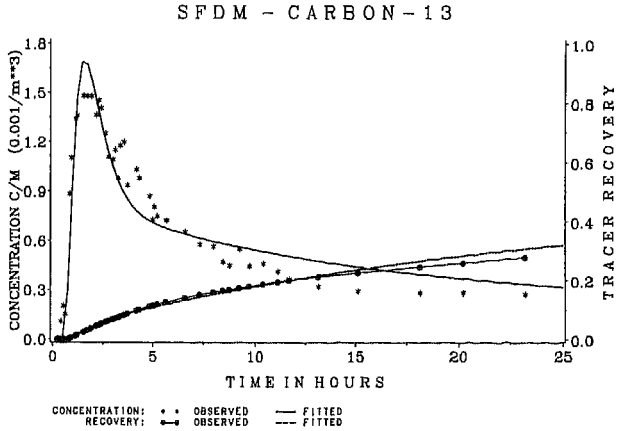

Fig. 10. Fitting of (6) for $H^{13}CO_3^-$ with additional fitting of the mass recovery curves (parameters given in Table 2).

The new fitting procedure still did not yield the same transit time of water, (t_o), from the D_2O and uranine tracer curves. The discrepancy cannot be explained in terms of $R_{af} > 1$, because an unreasonably high k_a value would then appear, which in turn would yield a high R_{ap} value. The origin of this discrepancy remains unknown. However, uranine is undoubtedly not an ideal tracer, though in this case the sorption effects are not strong enough to show which parameters play an important role.

The new model (equation (6)) enables a good fit of mass recoveries for both I^- and $H^{13}CO_3^-$, which was not obtainable for the model given by (12) with either $R_{af} = 1$ [*Maloszewski and Zuber*, 1989] or $R_{af} > 1$ (this work). However, it is not possible to determine five fitting parameters independently because of their interplay which is demonstrated by an example in Figure 9 and Table 2 for I^-, where the same good fit was obtained for two sets of parameters. Therefore for adsorable tracers (I^- and $H^{13}CO_3^-$), both t_o and Pe determined from the D_2O experiment were fixed as known parameters, and then $2b$ and n_p were fixed for finding the R_{ap} factor (see Table 2).

In the case of $H^{13}CO_3^-$, (6) improves the fit for the mass recovery curve at some cost of the concentration curve (compare Figures 6 and 10). It also confirms high and fast losses of that substance in comparison with I^- (k_1', k_1'/k_2, and R_{ap} distinctly greater than for I^-).

The fissure porosity n_f and fissure apertures $2b$ given in Table 2 do not differ essentially from those of Table 1, which means that in this case both (6) and (12) seem to yield fissure parameters, n_f and $2b$, satisfactorily, but (6) undoubtedly yields more proper values of matrix parameters. However, the upper range of the matrix porosity n_p presented in Table 2 for D_2O and I^- is evidently too high. Assuming that the transit times of water, t_o, given in Table 2 are more correct than those in Table 1, one has to accept the tortuosity factor in (16) as being close to 1.5 and reject the higher value. This rejection seems to be theoretically justified because in the derivation of (15) both the tortuosity resulting from the existence of the network of fissures and the tortuosity of particular fissures were already allowed for, leading to the power of the τ_f factor. In consequence the acceptance in our previous works of a possible experimental τ_f value equal to 2.5 in the model in which τ_f^2 appears was most probably in error because this value already results from the model, i.e., $\tau_f^2 = 1.5^2 = 2.5$. The lower range of the fissure porosity obtained from (14) under the assumption of $h = 32.8$ m (aquifer thickness) may also be questioned, and probably $h = 15$ m (length of screen in the pumping well) should be used as a more realistic value, which yields $n_f = 0.0027$. When $k_{10} = 4$ m/d, $\tau_f = 1.5$, and $n_f = 0.0027$ are used in (16) and (18), the fissure aperture determined from D_2O data is 250 μm, and matrix porosity is 0.39. This matrix porosity is

TABLE 2. Parameters Obtained From Equation (6) With Additional Fitting of the Recovery and Assuming $R_{af} = 1.0$

	Fitted Parameters					Calculated Parameters			
Tracer	t_0, hours	Pe^{-1}	a, hours$^{-1/2}$	k_1', hours^{-1}	k_2, hours^{-1}	n_f,[a] %	$2b$,[b] μm	n_p,[c] %	R_{ap}
D_2O	0.64	0.02	2.4	...	...	0.12–0.27	250–710	39–79	1.0[f]
Uranine	0.95	0.015	0.8	...	...	0.18–0.40	200–580	29–58	1.0[f]
I^-	0.80	0.02	1.9	0.06	0.01	0.15–0.34	220–640	36–73	1,0[f]
	0.64	0.02	2.5	0.05	0.007	0.12–0.27	250[d]	39[e]	1.7[g]
$H^{13}CO_3^-$	0.64	0.02	2.5	0.72	0.1	0.12–0.27	250[d]	39[e]	2.7[g]

[a] Equation (14) for $h = 15$–32.8 m.
[b] Equation (16).
[c] Equations (17) and (18).
[d] Taken as that value giving a reasonable n_p value for D_2O.
[e] Taken from D_2O data for $2b = 250$ μm.
[f] Assumed.
[g] Calculated from equation (9) with the aid of equation (17).

closer to the typical average value of matrix porosity (0.40) for chalks and marls than the values for D_2O given in Tables 1 and 2. However, such an interpretation for uranine yields matrix porosity values even smaller than the already low values given in Tables 1 and 2. In other words, the uranine behaves as if it were delayed in the fissures ($R_{af} > 1$) and not adsorbed in the matrix ($R_{ap} = 1$, $k_1 = k_2 = 0$). This phenomenon remains unclarified.

It should be remembered that for both I^- and $H^{13}CO_3^-$ the reaction "constants" are bulk parameters defined by the model and they do not supply information on the physical or chemical processes of the involved reactions. This restriction is especially true for the discussed substances, as *Behrens* [1985] for I^- and *Mozeto et al.* [1984] for $H^{13}CO_3^-$ proved that the behavior of both of these tracers in groundwater systems is very complex. On theoretical and experimental grounds, *Valocchi* [1986] concluded that in most cases the nonequilibrium effects are limited to a very fast flow close to pumping wells. On the other hand, *Mozeto et al.* [1984] found that in some cases $H^{13}CO_3^-$ was not equilibrated with the solid phase even after 800 hours. No definite conclusions in this respect can be drawn from the data of the present work, though the rate constants for $H^{13}CO_3^-$ presented in Table 2 suggest a dominant role of relatively fast nonequilibrium reactions; however, these reactions are not fast enough to treat $H^{13}CO_3^-$ as being in equilibrium.

Intrinsic Dispersivity and Its Relation to Rock Characteristics

The intrinsic dispersivity is defined here as that which would be observed in th case of no diffusion (n_p and/or $D_p = 0$) and no sorption. The interpretation performed above with the aid of (6) and (12) was based on a tacit assumption of negligible dispersion caused by nonideal injection. *Guvanasen and Guvanasen* [1987] showed that if the volume of injected tracer and chase fluids is spread too far around the injection well, the observed dispersivity increases. According to *Garnier et al.* [1985], tracer and chase fluid volumes were 0.06 m^3 for D_2O and $H^{13}CO_3^-$ and 0.10 m^3 for I^- and uranine. The length of the screened part of the injection well was 10 m, which for $n_f = 0.0027$ yields a radius of the injected volume of about 0.8–1.1 m. Even if a part of the injected fluid was initially left in the injection well (the well diameter was not reported by Garnier et al.), the estimated radius seems to be very large in comparison with the obtained dispersivity of about 0.2 m ($D/v = x\,Pe^{-1} = 10.22\ \text{m} \times 0.02 = 0.2$ m). Therefore it is necessary to consider how the nonideal injection influenced the obtained value of the dispersivity. Any additive distributions have additive variances. Thus

$$\sigma_t^2 = \sigma_{\text{inj}}^2 + \sigma_{\text{true}}^2 \tag{24}$$

where σ_t^2 is the total variance of the tracer concentration curve which would be observed in the case of nondiffusive and nonsorbable tracer, σ_{inj}^2 is the variance of the tracer distribution caused by a finite injection volume, and σ_{true}^2 is the variance caused by intrinsic dispersivity, uninfluenced by the nonideal injection. Assuming a rectangular shape of tracer distribution along the flow line at the time of injection, the space variance caused by the injection is easily obtained from the definition of variance which yields

$$\sigma_{\text{inj},x}^2 = R^2/3 \tag{25}$$

where R is the radius of the injected fluid volume. The time variance is

$$\sigma_{\text{inj}}^2 = \sigma_{\text{inj},x}^2/v^2 = t_o^2\sigma_{\text{inj},x}^2/x^2 = t_o^2R^2/(3x^2) \tag{26}$$

which for $R = 1.1$ m, $t_o = 0.64$ hour, and $x = 10.22$ m gives about 0.0016 hour^2. The total variance for the ordinary dispersion model (no diffusion and no sorption) is related to the Pe number by a well-known formula [e.g., *Kreft and Zuber*, 1978],

$$\sigma_t^2 = 2t_o^2\,Pe^{-1} \tag{27}$$

and equal here to 0.016 hour^2. The true variance caused by only intrinsic dispersivity is obtained then from (24),

$$\sigma_{\text{true}}^2 = 0.016 - 0.0016 = 0.014\ \text{hour}^2 \tag{28}$$

and the true Pe number is obtained by again applying (27),

$$Pe_{\text{true}}^{-1} = \sigma_{\text{true}}^2/(2t_o^2) = 0.018 \tag{29}$$

Obviously, the nonideal injection in that particular case had little influence on the observed value of the Peclet number and consequently on the obtained value of the intrinsic dispersivity. A low value of the intrinsic dispersivity suggests that the investigated system is not highly dispersive for hydrodynamic reasons. Consequently, the obtained dispersivity may serve for the estimation of the upper limit of the fissure distribution variance.

Flow of nonsorbable and nondiffusive tracer through a network of parallel fissures with a lognormal distribution of diameters or apertures having variance σ^2 produces a time tracer curve with variance given by [*Neretnieks*, 1983]

$$(\sigma_t/t_o)^2 = \exp\,[(2\ln 10)^2\sigma^2] - 1 \tag{30}$$

By comparing (30) and (27) and rearranging, one gets

$$\sigma^2 = \ln\,(1 + 2\,Pe^{-1})/(2\ln 10)^2 \tag{31}$$

If Pe is thought of as a measure of the fissure aperture distribution, (31) yields $\sigma^2 < 0.002$ for $Pe^{-1} = 0.018$, which means that the discussed distribution is rather narrow and, consequently, the single-fissure approximation should be particularly acceptable. It remains an open question how the single-fissure approximation works for systems of high intrinsic dispersivities, i.e., for systems having a broad distribution of fissure apertures, though examples given by *Maloszewski and Zuber* [1985] seem to indicate that such systems are also interpretable.

It is self-evident that (31) is applicable only if the intrinsic dispersivity is used. Models which treat the observed dispersivity as the result of fissure distribution, without considering the additional dispersion caused by matrix diffusion, are unacceptable and cannot yield consistent results (see Figures 1 and 11). In this respect some remarks on other models applied to the same tracer data, or to other tracer data obtained in the same experimental field, are unavoidable.

Garnier et al. [1985] interpreted the experimental curves shown in Figure 2 by the method of moments based on the ordinary dispersion model. Theoretically, if $n_p > 0$ and $D_p > 0$, neither the first nor the second moment exists for a single fissure, whereas experimentally, as a result of strong tailing

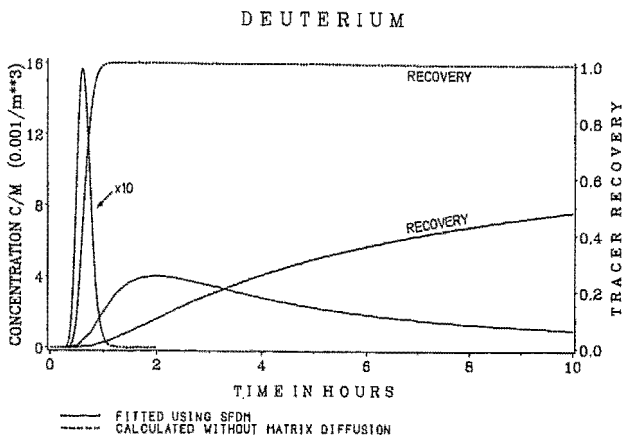

Fig. 11. Tracer and mass recovery curves for D_2O (solid lines) from Figure 7 compared with theoretical tracer curves (dashed) obtained for $t_o = 0.64$ hour, $Pe^{-1} = 0.02$ (intrinsic dispersivity), and $a = 0$ (i.e., tracer and mass recovery curves which would be observed in the case of zero matrix porosity).

effects, both moments are practically unmeasurable. Without a proper mathematical model, *Garnier et al.* [1985], though fully aware of the matrix diffusion effects, were unable to get the true values of parameters. The convective transit times (t_c in the discussed paper, t_o here) for particular tracers were estimated to be between 1.5 and 2.5 hours, and dispersivities between 0.74 and 1.02 m, which compare poorly with the intrinsic dispersivity of 0.2 m obtained here. In a later work, *Wang et al.* [1987], without mentioning matrix diffusion effects, interpreted the same experiment by choosing arbitrarily only the uranine tracer curve and arrived at dispersivities between 0.42 and 0.54 m. Undoubtedly, both *Garnier et al.* [1985] and *Wang et al.* [1987] wanted to obtain the intrinsic dispersivity (dispersivities estimated by Garnier et al. directly from the tracer curves were even 1 order of magnitude larger) and arrived at reasonable values by choosing the least diffusable tracer and rejecting the tailing part of the tracer curve. However, examples shown in Figures 1 and 11 prove that such an approach is in principle unacceptable. Figure 11 shows a comparison of concentration and mass recovery curves for the discussed experiment. The diffusion curves are those observed for D_2O (Figure 7), and the nondiffusive curves are those which would be observed in the case of n_p or $D_p = 0$. The diffusive curves interpreted by the SFDM have the same intrinsic dispersivity (0.2 m) as the nondiffusive curves, but their higher spread results from diffusion into the porous matrix. If these curves were interpreted by the ordinary dispersion model (i.e., dispersion equation without diffusion term for the matrix), the observed apparent dispersivity would differ from the intrinsic dispersivity and would not be a model parameter because its value would also depend on the scale of the experiment and flow velocity (or t_o). *Maloszewski and Zuber* [1985] have already pointed out that only if the a parameter is very low (i.e., either n_p is low or $2b$ large, or both) may the ordinary dispersion model be used for short-term experiments, but then only t_o and Pe are obtainable in approximation, and the information on the matrix parameters is lost.

In a recent paper, *Carlier* [1988] reported another tracer experiment performed in the same experimental field. Unfortunately, the experimental tracer curve was not presented, but from the data given in Table 1 of that paper one can guess that uranine or another, even less diffusable tracer was used. The model developed by Carlier does not take into account the diffusion of tracer into the matrix. Thus its use for the prediction of pollutant movement may lead to a serious error. In that particular case, as the experiment was very short and the tracer used was of a low-diffusion coefficient, the obtained mean transit time of the tracer was relatively close to the mean transit time of water, and the estimated dispersivity was also relatively close to the intrinsic dispersivity. Both would be far from the true mean travel time and dispersivity of a pollutant in a larger-scale movement, because then the diffusion into the matrix plays a dominant role, and the mean velocity of nonsorbable solute is $(n_p + n_f)/n_f$ times slower than the mean velocity of water [e.g., *Neretnieks*, 1980; *Maloszewski and Zuber*, 1984, 1985].

CONCLUSIONS

The model of a single fissure with a constant aperture undoubtedly differs from reality (see, for example, *Tsang and Tsang* [1987] for variations in fissure apertures). However, it works surprisingly well, as has already been shown for nonsorbable tracers in an earlier paper [*Maloszewski and Zuber*, 1985]. Within this work the model is extended to sorbable substances by adopting and incorporating the model of *Cameron and Klute* [1977], which couples an instantaneous equilibrium reaction governed by a linear adsorption isotherm with a nonequilibrium kinetic reaction of the first order. A new interpretational procedure, consisting of an additional fitting of theoretical mass recovery curves to experimental data, yields more reliable parameters than the fitting procedure applied so far. The model is shown to be applicable to short-term tracer experiments by yielding, for different tracers, consistent values of fitting parameters and reliable values of physical parameters from the interpretation of the multitracer experiment of *Garnier et al.* [1985], which involved two nonsorbable and two sorbable tracers. The experimental curves for the four different tracers differ considerably from one another, which means that not the channeling effect (different flow velocities in fissures with different apertures) but the diffusion into the matrix is the dominant process responsible for the observed spread of the tracer curves. If the channeling effect were dominant, the tracer curves for different tracers would not differ considerably. This argument seems to justify the applicability of the single-fissure dispersion model in short-term tracer experiments in densely fissured rocks. A further argument results from the comparison of the tracer curves obtained for nonsorbable and sorbable tracers. As the model works very well for nonsorbable tracers and only reasonably well for sorbable substances, it may be concluded that for a proper description of sorbable solute transport an adequate formulation of the reaction model is probably more important than the formulation of a fissure network.

The model developed within this work is probably the simplest one available for the solute transport in a fissure in a microporous matrix. However, even this simple model, in the case of sorbable substances, is characterized by a larger number of fitting parameters and even by a large number of physical parameters. In order to reduce the number of fitting

parameters and to obtain the values of physical parameters characterizing the sorption process it is necessary to determine some other parameters independently, for example, from an experiment with a nonsorbable tracer, as shown within this paper. Obviously, it is unreasonable to expect more sophisticated models, as for instance the one developed by *Tsang and Tsang* [1987], to be applicable for the interpretation of trace experiments, especially as it is difficult to see how the matrix diffusion can be incorporated into these models "with very little added effort" [*Tsang and Tsang*, 1987, p. 474]. Tsang and Tsang's model takes into account the real geometry of fissures and therefore must be characterized by a larger number of parameters, if diffusion and sorption are not neglected.

APPENDIX: THE SOLUTION OF TRANSPORT EQUATIONS (1)–(4)

By substituting (8) into (2) and defining

$$v' = v/R_{af} \tag{A1}$$

$$D' = D/R_{af} \tag{A2}$$

$$n_p' = n_p R_{ap}/R_{af} \tag{A3}$$

$$D_p' = D_p/R_{ap} \tag{A4}$$

(1)–(4) become

$$\frac{\partial c_f}{\partial t} + v' \frac{\partial c_f}{\partial x} - D' \frac{\partial^2 c_f}{\partial x^2} - \frac{n_p' D_p'}{b} \frac{\partial c_p}{\partial y}\bigg|_{y=b} = 0 \tag{A5}$$

$$\frac{\partial c_p}{\partial t} - D_p' \frac{\partial^2 c_p}{\partial y^2} + \frac{(1-n_p)\rho}{n_p R_{ap}} \frac{\partial q_2}{\partial t} = 0 \tag{A6}$$

$$\frac{\partial q_2}{\partial t} = \frac{n_p}{(1-n_p)\rho} k_1 c_p - k_2 q_2 \tag{A7}$$

Applying the Laplace transforms to (A5)–(A7) and next solving the transformed (A7) and substituting it into (A6), one gets, instead of (A6) and (A7),

$$s\left(1 + \frac{k_1'}{s+k_2}\right) \bar{c}_p - D_p' \frac{d^2 \bar{c}_p}{dy^2} = 0 \tag{A8}$$

where s is the Laplace variable with respect to time.

A general solution to (A8) is

$$\bar{c}_p = A_1 \exp[r_1(y-b)] + A_2 \exp[r_2(y-b)] \tag{A9}$$

where r_1 and r_2 are

$$r_{1,2} = \pm \left(\frac{s(s+k_2+k_1')}{(s+k_2)D_p'}\right)^{1/2} \tag{A10}$$

For the boundary conditions discussed earlier one gets

$$\bar{c}_p = \bar{c}_f \exp\left[-\left(\frac{s(s+k_2+k_1')}{(s+k_2)D_p'}\right)^{1/2}(y-b)\right] \tag{A11}$$

$$\left.\frac{d\bar{c}_p}{dy}\right|_{y=b} = -\bar{c}_f \left(\frac{s(s+k_2+k_1')}{(s+k_2)D_p'}\right)^{1/2} \tag{A12}$$

Equation (A12) substituted into the transformed (A5) gives

$$\frac{d^2\bar{c}_f}{dx^2} - \frac{v'}{D'}\frac{d\bar{c}_f}{dx} - \left[\frac{n_p'D_p'}{bD'}\left(\frac{s(s+k_2+k_1')}{(s+k_2)D_p'}\right)^{1/2} + \frac{s}{D'}\right]\bar{c}_f = 0 \tag{A13}$$

which has a general solution given by

$$\bar{c}_f = A_3 \exp(r_3 x) + A_4 \exp(r_4 x) \tag{A14}$$

where r_3 and r_4 are the square roots of the equation

$$r^2 - \frac{v'}{D'} r - \left[\frac{n_p'D_p'}{bD'}\left(\frac{s(s+k_2+k_1')}{(s+k_2)D_p'}\right)^{1/2} + \frac{s}{D'}\right] = 0 \tag{A15}$$

and are represented by

$$r_{3,4} = \frac{v'}{2D'} \pm \frac{v'}{2D'} \cdot \left\{1 + \frac{4D'}{(v')^2}\left[\frac{n_p(D_p)^{1/2}}{b}\left(\frac{s(s+k_2+k_1)}{s+k_2}\right)^{1/2} + s\right]\right\}^{1/2} \tag{A16}$$

Applying the boundary conditions and $v'/D' = v/D$, one gets

$$\bar{c}_f(s) = \frac{M}{Q}\exp\left(\frac{vx}{2D}\right) \cdot \exp\left\{-\frac{vx}{2D}\left[1 + \frac{4D'}{(v')^2}\left(s + 2a\left(s + \frac{sk_1'}{s+k_2}\right)^{1/2}\right)\right]^{1/2}\right\} \tag{A17}$$

Equation (A17) is the Laplace transform of the sought solution for the tracer concentration in water outflowing at the end of the fissure. Obtaining the inverse can be made easier by applying the following expression [*Gradshteyn and Ryzhik*, 1980]:

$$\exp(-\theta) = (2/\pi^{1/2})\int_0^\infty \exp[-\beta^2 - (0.5\theta/\beta)^2]\, d\beta \tag{A18}$$

where $(-\theta)$ is the argument of the second exponential in (A17). By substituting (A18) for the second exponential in (A17), applying $s' = s + k_2$ and $t_o' = x/v'$, and rearranging, one gets

$$\bar{c}_f(s) = \frac{M}{Q}\frac{2}{\pi^{1/2}}\exp\left(\frac{vx}{2D}\right) \cdot \int_0^\infty \exp\left[-\beta^2 - \frac{vx}{4D\beta^2}\left(\frac{vx}{4D} - k_2 t_o'\right)\right] \cdot \exp\left[-\frac{vx}{4D\beta^2} t_o' s' - \frac{vx}{2D\beta^2} a t_o' \cdot \left(s' - \frac{k_1'k_2}{s'} + k_1' - k_2\right)^{1/2}\right] d\beta \tag{A19}$$

The inverse transform can be found similarly as in the work by *Klotz et al.* [1988] by applying the inverse of the following imaginary function [*Carnahan and Remer*, 1984]:

$$F(s) = \exp\{-\eta[s + \beta_1 - \beta_2/(s + \beta_3)]^{1/2}\} \quad \text{(A20)}$$

which is

$$f(t) = \frac{\eta}{(4\pi t^3)^{1/2}} \exp\left(-\frac{\eta^2}{4t} - \beta_1 t\right) + \frac{\eta}{2}\left(\frac{\beta_2}{\pi}\right)^{1/2} \cdot \exp(-\beta_3 t) \int_0^t \exp\left[-\frac{\eta^2}{4\tau} - (\beta_1 - \beta_3)\tau\right] \cdot I_1\{2[\beta_2\tau(t-\tau)]^{1/2}\} \frac{d\tau}{\tau(t-\tau)^{1/2}} \quad \text{(A21)}$$

where I_1 is the modified Bessel function of the first kind of the first order. Now by making use of the following properties of the Laplace transforms,

$$F(s + \alpha) \stackrel{\triangle}{=} f(t)\exp(-\alpha t) \quad \text{(A22)}$$

$$F(s)\exp(-\omega s) \stackrel{\triangle}{=} f(t) \qquad t > \omega$$
$$F(s)\exp(-\omega s) \stackrel{\triangle}{=} 0 \qquad t < \omega \quad \text{(A23)}$$

and taking $\omega = vxt_o'/(4D\beta^2)$, which gives for $t > \omega$

$$\beta > [vxt_o'/(4Dt)]^{1/2} \quad \text{(A24)}$$

and inserting

$$\alpha = k_2 \quad \text{(A25)}$$

$$\eta = vxat_o'/(2D\beta^2) \quad \text{(A26)}$$

$$\beta_1 = k_1' - k_2 \quad \text{(A27)}$$

$$\beta_2 = k_1'k_2 \quad \text{(A28)}$$

$$\beta_3 = 0 \quad \text{(A29)}$$

one obtains, after changing the integration variable and rearranging, the final solution given by (6).

NOTATION

D dispersion coefficient in fissures, L^2/T.
D' reduced dispersion coefficient (equation (A2)), L^2/T.
D_p coefficient of molecular diffusion in stagnant water in matrix, L^2/T.
D_p' reduced coefficient of molecular diffusion in stagnant water in matrix (equation (A4)), L^2/T.
D_v coefficient of diffusion in free water, L^2/T.
D/v intrinsic dispersivity in fissures, L.
$D/(vx)$ dispersion parameter, equal to $1/Pe$.
K permeability coefficient, L^2.
M mass or activity injected, M or Bq.
Pe Peclet number, equal to vx/D.
Q volumetric flow rate through system (pumping rate), L^3/T.
R radius of the volume occupied by injected fluid, L.
R_{af} retardation factor caused by instantaneous equilibrium sorption in fissure.
R_{ap} retardation factor caused by instantaneous equilibrium sorption in matrix.
a fitting parameter given by (9) or (13), $T^{-1/2}$.
b half-fissure aperture, L.
c_f tracer concentration in water in fissures, M/L^3 or Bq/L^3.
c_p tracer concentration in water in matrix, M/L^3 or Bq/L^3.
d_c diameter of capillaries in matrix, L.
h thickness of aquifer, L.
k_a distribution coefficient for tracer concentration in solid phase expressed per unit rock surface, L.
k_d distribution coefficient, L^3/M.
k_3 distribution coefficient for instantaneous equilibrium in matrix, L^3/M.
k_1 forward rate constant, T^{-1}.
k_1' reduced forward rate constant (equation (7)), T^{-1}.
k_2 backward rate constant, T^{-1}.
k_{10} hydraulic conductivity at 10°C expressed in m/d, L/T.
n_f fissure porosity.
n_p matrix porosity.
n_p' reduced matrix porosity (equation (A3)).
q_1 tracer concentration in solid phase governed by instantaneous equilibrium, M/M or Bq/M.
q_2 tracer concentration in solid phase governed by first-order nonequilibrium kinetic reaction, M/M or Bq/M.
q_s tracer concentration in solid phase expressed per unit rock surface, M/L^2 or Bq/L^2.
r_i mean grain radius of ith fraction of grain size curve, L.
t time variable, T.
t_o mean transit time of water, T.
t_o' reduced mean transit time of water (equation (11)), T.
v mean flow velocity, L/T.
v' reduced mean flow velocity (equation (A1)), L/T.
x distance at which tracer is measured, L.
y space coordinate perpendicular to fissure extension, L.
δ constrictivity factor.
ν_i weight fraction of ith fraction of grain size curve.
ρ density of the matrix material, M/L^3.
σ^2 variance of fissure apertures in lognormal distribution.
σ^2_{inj} time variance of tracer distribution caused by nonideal injection, T^2.
$\sigma^2_{inj,x}$ space variance of tracer distribution caused by nonideal injection, L^2.
σ_t^2 total time variance of tracer distribution in case of no diffusion into matrix and no adsorption, T^2.
σ^2_{true} time variance of tracer distribution caused by intrinsic dispersivity only, T^2.
τ_f tortuosity factor for fissures.
τ_p tortuosity factor for micropores.
Φ_1 mass transfer of solute (tracer) between liquid and solid phases in matrix governed by linear adsorption isotherm and instantaneous equilibrium, T^{-1} or Bq$M^{-1}T^{-1}$.
Φ_2 mass transfer of solute (tracer) between liquid and solid phases in matrix governed by first-order nonequilibrium kinetic reaction, T^{-1} or Bq$M^{-1}T^{-1}$.

Acknowledgments. This work was performed at GSF–Institut für Hydrologie, with a partial support to A.Z. from the Polish Academy of Sciences under CPBP 03.02.

REFERENCES

Behrens, H., Speciation of radioiodine in aquatic and terrestrial systems under the influence of biogeochemical processes, in *Speciation of Fission and Activation Products in the Environment*, pp. 223–230, Elsevier, New York, 1985.

Cameron, D. R., and A. Klute, Convective-dispersive solute transport with a combined equilibrium and kinetic adsorption model, *Water Resour. Res.*, *13*, 183–188, 1977.

Carlier, E., Nouvelles équations de propagation d'un pollutant dans une nappe souterraine, *J. Hydrol. Amsterdam*, *103*, 189–197, 1988.

Carnahan, C. L., and J. S. Remer, Nonequilibrium and equilibrium sorption with a linear sorption isotherm during mass transport through an infinite porous medium: Some analytical solutions, *J. Hydrol. Amsterdam*, *73*, 227–258, 1984.

Freeze, J. A., and J. F. Cherry, *Groundwater*, Prentice-Hall, Englewood Cliffs, N. J., 1979.

Garnier, J. M., N. Crampon, C. Preaux, G. Porel, and M. Vreulx, Traçage par ^{13}C, ^{2}H, I^- et uranine dans la nappe de la craie sénonienne en écoulement radial convergent (Béthune, France), *J. Hydrol. Amsterdam*, *78*, 379–392, 1985.

Gradshteyn, I. S., and I. M. Ryzhik, *Table of Integrals, Series and Products*, Academic, San Diego, Calif., 1980.

Grisak, G. E., and J. F. Pickens, Solute transport through fractured media, 1, The effect of matrix diffusion, *Water Resour. Res.*, *16*, 719–730, 1980.

Grisak, G. E., J. F. Pickens, and J. A. Cherry, Solute transport through fractured media, 2, Column study of fractured till, *Water Resour. Res.*, *16*, 731–739, 1980.

Guvanasen, V., and V. M. Guvanasen, An approximate semianalytical solution for tracer injection test in a confined aquifer with a radially converging flow field and finite volume of tracer and chase fluid, *Water Resour. Res.*, *23*, 1607–1619, 1987.

Klotz, D., P. Maloszewski, and H. Moser, Mathematical modeling of radioactive tracer migration in water flowing through saturated porous media, *Radiochim. Acta*, *44/45*, 373–379, 1988.

Kreft, A., and A. Zuber, On the physical meaning of the dispersion equation and its solutions for different initial and boundary conditions, *Chem. Eng. Sci.*, *33*, 1471–1480, 1978.

Kreft, A., and A. Zuber, Comments on "Flux-averaged and volume-averaged concentrations in continuum approaches to solute transport" by J. C. Parker and M. Th. van Genuchten, *Water Resour. Res.*, *22*, 1157–1158, 1986.

Lenda, A., and A. Zuber, Tracer dispersion in groundwater experiments, in *Isotope Hydrology 1970*, pp. 619–641, International Atomic Energy Agency, Vienna, Austria, 1970.

Maloszewski, P., and A. Zuber, Interpretation of artificial and environmental tracers in fissured rocks with a porous matrix, in *Isotope Hydrology 1983*, pp. 635–651, International Atomic Energy Agency, Vienna, Austria, 1984.

Maloszewski, P., and A. Zuber, On the theory of tracer experiments in fissured rocks with a porous matrix, *J. Hydrol. Amsterdam*, *79*, 333–358, 1985.

Maloszewski, P., and A. Zuber, Mathematical models for interpreting tracer experiments in fissured aquifers, in *The Application of Isotope Techniques in the Study of the Hydrogeology of Fractured and Fissured Rocks*, pp. 287–301, International Atomic Energy Agency, Vienna, Austria, 1989.

Maloszewski, P., S. Witczak, and A. Zuber, Prediction of pollutant movement in groundwaters, in *Nuclear Techniques in Groundwater Pollution Research*, pp. 61–81, International Atomic Energy Agency, Vienna, Austria, 1980.

Mozeto, A. A., P. Fritz, and E. J. Reardon, Experimental observations on carbon isotope exchange in carbonate-water systems, *Geochim. Cosmochim. Acta*, *48*, 495–504, 1984.

Neretnieks, I., Diffusion in the rock matrix: An important factor in radionuclide retardation?, *J. Geophys. Res.*, *85*(B8), 4379–4397, 1980.

Neretnieks, I., A note on fracture flow dispersion mechanism in the ground, *Water Resour. Res.*, *19*, 364–370, 1983.

Pirson, S. J., *Handbook of Well Log Analysis*, Prentice-Hall, Englewood Cliffs, N. J., 1963.

Saffman, P. G., Dispersion in flow through a network of capillaries, *Chem. Eng. Sci.*, *11*, 125–129, 1959.

Skagius, K., and I. Neretnieks, Porosities and diffusivities of some nonsorbing species in crystalline rocks, *Water Resour. Res.*, *22*, 389–398, 1986.

Sudicky, E. A., and E. O. Frind, Contaminant transport in fractured porous media: Analytical solutions for a system of parallel fractures, *Water Resour. Res.*, *18*, 1634–1642, 1982.

Tsang, Y. W., and C. F. Tsang, Channel model of flow through fractured media, *Water Resour. Res.*, *23*, 467–479, 1987.

Valocchi, A. J., Effect of radial flow on deviations from local equilibrium during sorbing solute transport through homogeneous soils, *Water Resour. Res.*, *22*, 1693–1701, 1986.

Wang, H. Q., N. Crampon, S. Huberson, and J. M. Garnier, A linear graphical method for determining hydrodispersive characteristics in tracer experiments with instantaneous injection, *J. Hydrol. Amsterdam*, *95*, 143–154, 1987.

Zuber, A., Theoretical possibilities of the two-well pulse method, in *Isotope Techniques in Groundwater Hydrology*, vol. II, pp. 277–294, International Atomic Energy Agency, Vienna, Austria, 1974.

P. Maloszewski, GSF–Institut für Hydrologie, Ingolstaedter Landstrasse 1, D-8042 Neuherberg, Federal Republic of Germany.

A. Zuber, Institute of Nuclear Physics, Radzikowskiego 152, PL-31342 Cracow, Poland.

(Received July 31, 1989;
revised January 20, 1990;
accepted January 31, 1990.)